

Thermopiezoelectric effects on optoelectronic properties of CdTe/ZnTe quantum wires

Sunil R. Patil** and R. V. N. Melnik*

M²NeT Lab, Wilfrid Laurier University, 75, University Ave. W, Waterloo, ON, N2L 3C5, Canada

Received 30 August 2008, accepted 21 October 2008

Published online 23 April 2009

PACS 46.25.Hf, 73.21.Hb, 77.65.-j, 85.60.-q

* Corresponding author: e-mail rmelnik@wlu.ca, Phone: +1 519 884 1970, Fax: +1 519 884 9738

** e-mail spatil@wlu.ca, Phone: +1 519 884 1970, Fax: +1 519 884 9738

We investigate thermopiezoelectric field distributions and their effects on electronic properties of the highly strained CdTe/ZnTe quantum wires. The full 3D coupled thermoelectromechanical formulation, consisting of balance equations for heat transfer, electrostatics and the mechanical field, is developed. Effects of thermal loadings on piezoelectric fields are determined for rectangular CdTe/ZnTe quantum wire systems. The conduction band edge shifts due to thermoelectromechanical loadings are calculated. A single band

Schrödinger equation is used to determine eigenstates for electrons and the analysis of classical effects are presented. Piezoelectric quantities are observed to be relatively less sensitive to thermal loadings. However, these effects are observed to be important in the determination of electronic/optoelectronic properties of quantum wire systems. The results presented here help improve our understanding of the classical effects on electronic structures and optoelectronic properties of CdTe/ZnTe quantum wires.

© 2009 WILEY-VCH Verlag GmbH & Co. KGaA, Weinheim

1 Introduction Wide band gap semiconductors have attracted much attention due to their potential applications in short wavelength optoelectronic devices. Currently, III–V GaN-based materials are leading materials for the fabrication of blue-green light emitting devices [1]. However, GaN-based low dimensional structures are found to have relatively high carrier densities to generate optical gain. This is due to the giant internal electric field as a result of misfit-strain induced piezoelectric and spontaneous polarization effects [2, 3]. To resolve higher carrier density problem in generating optical gain, II–VI ZnSe and CdTe-based nanostructures are the leading alternatives [4]. Recent advances in growth technologies of II–VI semiconductors now permit to grow high quality heterostructures [5]. Thus, with current progress in II–VI semiconductors, corresponding theoretical studies become very important. Among II–VI semiconductors, the CdTe/ZnTe system has become particularly interesting due to its potential to operate in the green region of spectrum and serve as an alternative to GaN-based systems [1, 6, 7].

CdTe quantum wires (QWRs) hosted by ZnTe matrix is a highly strained system (misfit $\approx 6\%$ [1, 6, 7]). It provides an ideal opportunity to analyse the influence of strain

and strain-induced piezoelectric effects on corresponding electronic/optoelectronic properties. On the other hand, it is found that the exciton binding energy is significantly reduced with increasing temperature and its effect is more important on the ground state energy than on the binding energy in CdTe/ZnTe nanostructures [8]. Other effects, such as relative stability of phases and phase transitions, can also be important in studying properties of nanostructures [9–11]. In addition, there are also many practical situations where interaction of thermopiezoelectric bodies with other media such as acoustic and fluid [12, 13] needs to be accounted for and the present formulation can act as a foundation for study of the resulting coupled models in the context of nanostructures. The study of fully coupled thermoelectromechanical effects in QWRs has both technological as well as fundamental interest.

In this paper, a 3D strongly coupled thermopiezoelectric model is formulated for zincblende (ZB) nanocrystals. Our major focus is on the thermal loading effect on piezoelectric properties and its influence on the optoelectronic properties of the CdTe QWR embedded in ZnTe matrix. We further study thermal loading effects on conduction band edge shifts and also determine the eigenstates for electrons. The

Schrödinger equation for single conduction band is used to determine the eigenstates for electrons and the analysis of classical effects is presented.

2 Theoretical formulations A mathematical model is formulated in order to study thermoelectromechanical effects in QWRs. A three dimensional (3D), linear model is developed with coupled multi-physics governing equations.

2.1 Thermopiezoelectric formulation The 3D linear fundamental equations for the thermoelectromechanical body occupying volume Ω , under steady state conditions, in our case can be summarized as follows [14, 15]:

$$\nabla \cdot \sigma = F, \quad \nabla \cdot D = q. \quad (1)$$

Here σ is stress tensor and D is electric displacement vector, F and q are mechanical body force and electric charge in Ω , respectively. Note that, at the thermal equilibrium, the temperature change becomes spatially independent and the problem is governed by the Eq. (1) only. Further, the explicit forms of constitutive relations relating thermoelectromechanical quantities are expressed for ZB nanostructures in Cartesian coordinates as follows:

$$\begin{aligned} \sigma_{xx} &= c_{11}\varepsilon_{xx} + c_{12}\varepsilon_{yy} + c_{12}\varepsilon_{zz} - \beta_1 T, \\ \sigma_{yy} &= c_{12}\varepsilon_{xx} + c_{11}\varepsilon_{yy} + c_{12}\varepsilon_{zz} - \beta_2 T, \\ \sigma_{zz} &= c_{12}\varepsilon_{xx} + c_{12}\varepsilon_{yy} + c_{11}\varepsilon_{zz} - \beta_3 T, \\ \sigma_{xy} &= 4c_{44}\varepsilon_{xy} - e_{14}E_z, & \sigma_{yz} &= 4c_{44}\varepsilon_{yz} - e_{14}E_x, \\ \sigma_{zx} &= 4c_{44}\varepsilon_{zx} - e_{14}E_y, & D_x &= e_{14}\varepsilon_{yz} + \chi_{11}E_x, \\ D_y &= e_{14}\varepsilon_{zx} + \chi_{11}E_y, & D_z &= e_{14}\varepsilon_{xy} + \chi_{33}E_z. \end{aligned} \quad (2)$$

Here c_{ij} , e_{ij} , χ_{ij} and β_i are elastic moduli, piezoelectric constants, dielectric constants and stress-temperature material constants, respectively, ε , E and T are strain tensor, electric field and temperature, respectively.

Normally, QWR related calculations are performed with a 2D formulation. However, piezoelectric coupling, which appears through shear components in ZB crystals [16] requires to solve this problem using a 3D model.

2.2 Schrödinger equation In order to study electronic properties of CdTe/ZnTe QWRs we use the Schrödinger equation for single conduction band. The thermopiezoelectric effects modify the potential energy term. The Schrödinger equation and effective potential are given as follows (electron is considered as a particle with effective mass m_c^* experiencing effective potential, V_c):

$$\begin{aligned} \nabla \cdot \left\{ -\frac{\hbar^2}{2m_c^*} \nabla \psi \right\} + V_c \psi &= E \psi, \\ V_c &= r \cdot E_g + a_c (\varepsilon_{xx} + \varepsilon_{yy} + \varepsilon_{zz}) - eV - \frac{\alpha_T T^2}{\beta_T + T}, \end{aligned} \quad (3)$$

Table 1 Physical parameters used for calculations.

material constants	CdTe	ZnTe
c_{11} (GPa)	53.8 ^a	72.2 ^b
c_{12} (GPa)	37.4 ^a	40.9 ^b
c_{44} (GPa)	20.18 ^a	30.8 ^b
e_{14} (C/m ²)	0.084 [20]	0.028 [21]
χ_{11}	10.4 [22]	10.3 [23]
β_1 (Pa/K)	97205.65 ^c	-73220.34 ^c
r	0.75 ^d	0.25 ^d
a_c (eV)	-1.8 ^d	-3.5 ^d
E_g (eV)	1.606 ^d	2.394 ^d
α_T (eV/K)	0.4357×10^{-3} [17]	0.467×10^{-3} [24]
β_T (K)	183.3 [17]	168 [24]

^a Ref. [18], ^b Ref. [19], ^c Calculated, ^d Ref. [1].

where ψ is the wave function and E is corresponding eigenvalue, r , a_c and e are band offset ratio, conduction band deformation potential and electronic charge respectively, E_g and V are the band gap and electric potential respectively, α_T and β_T are the Varshni coefficients [17].

The physical parameters used in this calculation are given in Table 1.

3 Results and discussion The calculations are performed using finite element method. The domain is meshed with quadratic triangular elements and the resulting algebraic eigenvalue problem is solved numerically overcoming known difficulties [26]. As shown in Fig. 1a, a rectangular CdTe QWR of dimensions $10 \times 10 \times 70$ nm is embedded in the $40 \times 40 \times 150$ nm ZnTe barrier. The lattice mismatch in CdTe/ZnTe QWR is $\varepsilon_0 = 5.89\%$.

Figure 1b shows ε_{xx} in (x,y) -plane. The magnitude of strain component ε_{xx} is observed to be less than about 3.45% ($\sim \varepsilon_0/2$) at all points inside the QWR, except for the region near the edges where the strain has higher magnitude than $\varepsilon_0/2$. The QWR causes the surrounding matrix to become strained and the strain decays slowly to zero away from the QWR. However, the qualitative strain distribution for square QWR differs from the one obtained from the Eshelby formulation. This is due to the assumption of isotropy of the QWR system in the latter [25, 27]. The hydrostatic strain component ($\varepsilon_{xx} + \varepsilon_{yy} + \varepsilon_{zz}$) relaxes to $\sim 3.65\%$ from unrelaxed state 17.67% ($= 3\varepsilon_0$) [28]. Thus significant strain relaxation occurs over most of the wire area. The magnitude of the hydrostatic strain component is particularly important as it leads to the rigid shift in electronic band structure [27].

Figure 2 shows a) electric potential and b) x -component of electric field in the x,y -plane. The potential difference across the QWR ends is ~ 0.08 V, which is smaller by order of magnitude as compared to GaN (~ 2 V) [28, 29]. The magnitude of the electric field exceeds 5 MV/m near the edges of the QWR and has the magnitude in fractions of MV/m inside the QWR. This is again a very small magnitude of electric field as compared to GaN (~ 600 MV/m) [28, 29]. The smaller magnitudes of electric

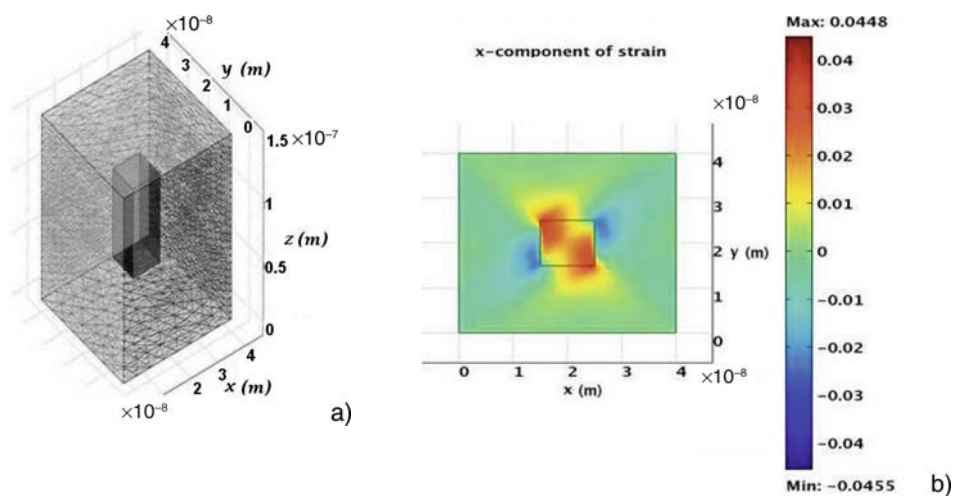


Figure 1 (online colour at: www.pss-a.com) a) 3D QWR geometry and meshing, b) ϵ_{xx} in (x,y) -plane.

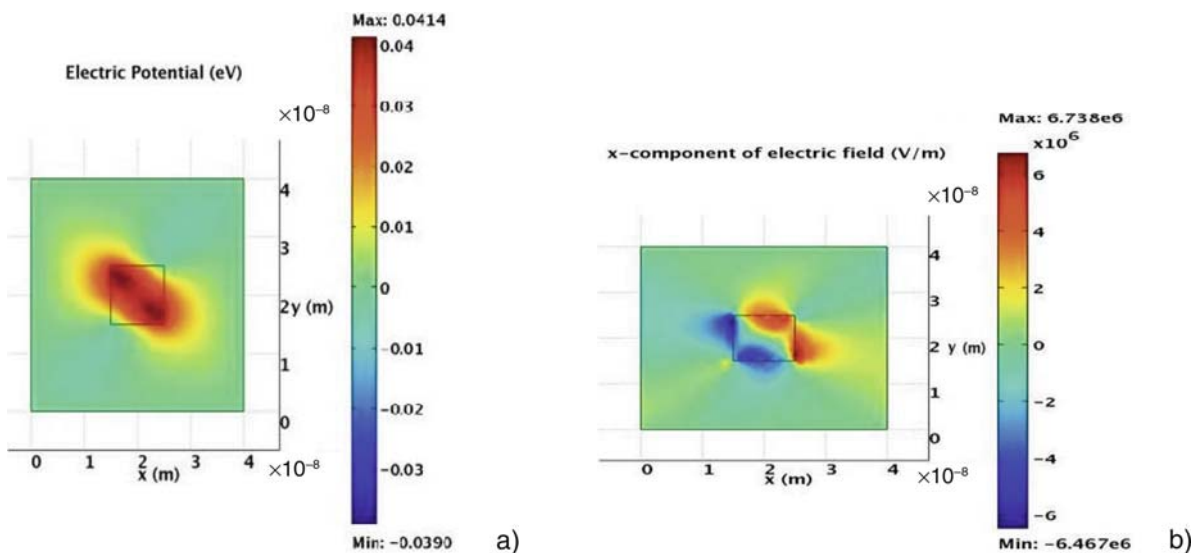


Figure 2 (online colour at: www.pss-a.com) a) Electric potential, b) x-component of electric field in (x,y) -plane.

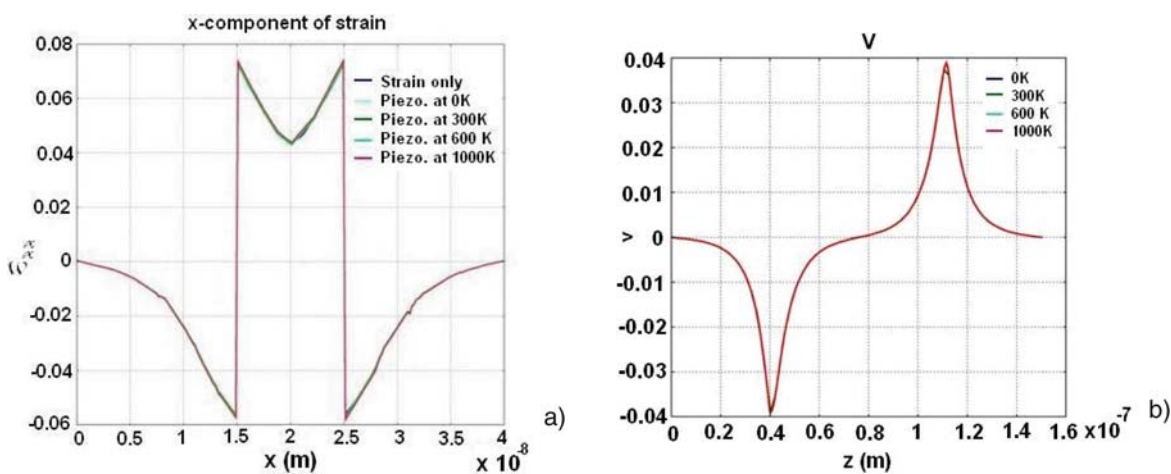


Figure 3 (online colour at: www.pss-a.com) a) ϵ_{xx} and b) electric potential as a function of thermopiezoelectric effects.

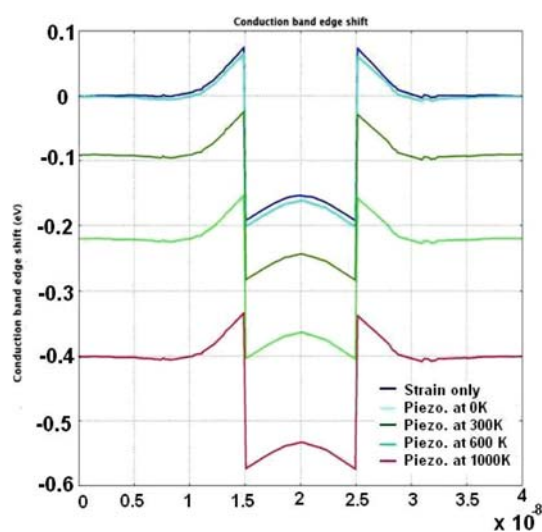


Figure 4 (online colour at: www.pss-a.com) Conduction band edge shifts against thermal loadings.

potential and electric field represent an advantage of CdTe based nanostructures over GaN as the latter structures face a problem of higher carrier density for generating optical gain [2].

Figure 3 shows a) ϵ_{xx} along x -direction and b) electric potential along z -direction as a function of thermopiezoelectric effects. The electromechanical parameters for the CdTe/ZnTe system are relatively less sensitive to temperature than those of GaN/AlN. This can be attributed to the low values of stress-temperature coefficients and relatively weak electromechanical coupling in CdTe/ZnTe compared to the GaN/AlN system. This also provides an added advantage to CdTe/ZnTe over GaN based nanostructures related to the thermal stability of piezoelectric quantities which may result in more stable optical properties.

Figure 4 shows the conduction band edge shifts in the CdTe/ZnTe QWR vs. thermal loadings from 0 K to 1000 K. The conduction band edge shifts at lower temperature are positive (~ 7 meV at 0 K inside the QWR), indicating an increase in effective band gap. However, as temperature increases band gap shifts become negative (~ -55 meV at 1000 K inside the QWR). The band gap shifts range from blue shift at low temperature to red shift at higher temperatures. The band gap shifts take peak values at the edges. In the ZnTe matrix, outside the QWR, conduction band edge shifts show similar trends. The conduction band edge shift at the operating temperature of 300 K is small (~ 27 meV). Hence, we conclude that the CdTe/ZnTe QWR system is more stable with respect to thermopiezoelectric effects compared to other similar materials such as GaN.

Figure 5 shows eigenenergies as functions of different classical effects in a conduction band of CdTe QWR. The electron eigenvalues corresponding to the ground state become smaller if we account for strain and piezoelectric effects. Piezoelectric effects lead to a significant change in

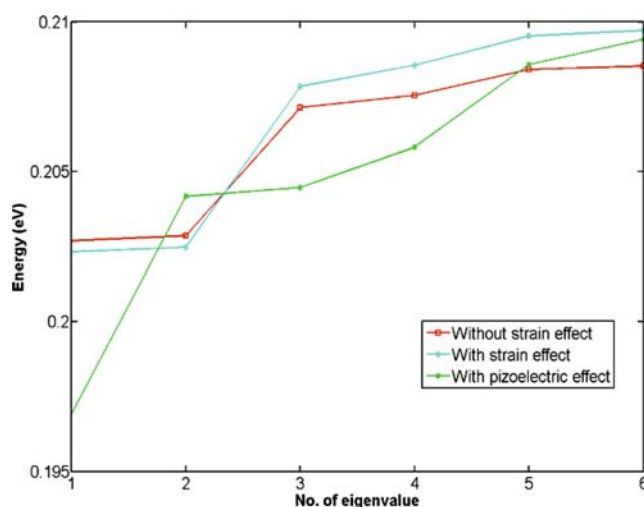


Figure 5 (online colour at: www.pss-a.com) Influence of classical effects on eigenenergies in CdTe/ZnTe QWRs.

ground state eigenvalues. However, eigenenergies corresponding to excited states are much less affected. The ground state eigenvalue without any electromechanical loading for CdTe/ZnTe is 0.203 eV which further decreases to 0.2025 eV and 0.197 eV with incorporation of strain and piezoelectric effects, respectively. This change in ground state eigenvalues may lead to change of optoelectronic properties.

4 Conclusions Full 3D strongly coupled thermoelectromechanical calculations have been carried out for CdTe/ZnTe quantum wires. The results indicate that CdTe based nanostructures have several advantages over their GaN counterparts, in particular with respect to the carrier density in generating optical gain. Thermally less sensitive electromechanical properties of CdTe/ZnTe may lead to thermally more stable performance which is important in preserving superior optoelectronic properties of nanostructures.

Acknowledgements This work, conducted in the M²NeT Laboratory (<http://www.m2netlab.wlu.ca>), was made possible by the facilities of the SHARCNET. R.M. acknowledges the support from the NSERC and CRC programs.

References

- [1] J. T. Woo et al., *J. Appl. Phys.* **102**, 033521 (2007).
- [2] F. Bernardini, V. Fiorentini, and D. Vanderbilt, *Phys. Rev. B* **56**, R10024 (1997).
- [3] M. Willatzen et al., *J. Appl. Phys.* **100**, 024302 (2006).
- [4] M. V. Maksimov et al., *Semiconductors* **31**, 800 (1997).
- [5] C. Onodera, T. Shoji, Y. Hiratate, and T. Taguchi, *Jpn. J. Appl. Phys.* **46**, 248 (2007).
- [6] T. W. Kim et al., *Appl. Phys. Lett.* **83**, 4235 (2003).
- [7] E. E. Onishchenko et al., *Physica E* **26**, 153 (2005).
- [8] A. E. Moussaouya, D. Briab, and A. Nougouai, *Sol. Energy Mater. Sol. Cells* **90**, 1403 (2006).

- [9] S. G. C. Moreira et al., *Appl. Phys. Lett.* **91**, 021101 (2007).
- [10] B. Wen and R. V. N. Melnik, *Appl. Phys. Lett.* **92**, 261911 (2008).
- [11] B. Wen and R. Melnik, *Chem. Phys. Lett.* **466**, 84 (2008).
- [12] R. V. N. Melnik, *Math. Comput. Simul.* **61**, 497 (2003).
- [13] H. Kamath et al., *Ultrasonics* **44**, 64 (2006).
- [14] R. V. N. Melnik, *Comput. Phys. Commun.* **142**, 231 (2001).
- [15] R. V. N. Melnik, *Int. Commun. Heat Mass Transfer* **30**, 83 (2003).
- [16] R. Melnik and R. Mahapatra, *Comput. Struct.* **85**, 698 (2007).
- [17] U. Pal et al., *Mater. Sci. Eng. B* **42**, 297 (1996).
- [18] R. D. Greenough and S. B. Palmer, *J. Phys. D, Appl. Phys.* **6**, 587 (1973).
- [19] M. Yamada, K. Yamamoto, and K. Abe, *J. Phys. D, Appl. Phys.* **10**, 1309 (1977).
- [20] J. Baars and F. Sorger, *Solid State Commun.* **10**, 875 (1972).
- [21] H. D. Riccius, *J. Appl. Phys.* **39**, 4381 (1968).
- [22] M. B. Kanoun et al., *Semicond. Sci. Technol.* **19**, 1220 (2004).
- [23] D. Berlincourt, H. Jaffe, and L. R. Shiozawa, *J. Appl. Phys.* **39**, 4381 (1968).
- [24] R. Passler et al., *J. Appl. Phys.* **86**, 4403 (1999).
- [25] J. R. Downes, D. A. Faux, and E. P. O'Reilly, *J. Appl. Phys.* **82**, 3754 (1997).
- [26] R. V. N. Melnik, *Eng. Comput.* **17**, 386 (2000).
- [27] J. R. Downes, D. A. Faux, and E. P. O'Reilly, *Mater. Sci. Eng. B* **35**, 357 (1995).
- [28] D. P. Williams, A. D. Andreev, and E. P. O'Reilly, *Phys. Rev. B* **73**, 241301 (2006).
- [29] S. R. Patil and R. V. N. Melnik, *Nanotechnology* **20**, 125402 (2009).